BIOCHEMISTRY
including biophysical chemistry & molecular biology

Article

pubs.acs.org/biochemistry

A Conserved Aromatic Residue Regulating Photosensitivity in Short-Wavelength Sensitive Cone Visual Pigments

Colleen M. Kuemmel,[†] Megan N. Sandberg,[‡] Robert R. Birge,*[,‡] and Barry E. Knox*[,†]

[†]Departments of Neuroscience and Physiology, Biochemistry and Molecular Biology, and Ophthalmology, SUNY Upstate Medical University, Syracuse, New York 13210, United States

[‡]Departments of Chemistry and Molecular and Cell Biology, University of Connecticut, Storrs, Connecticut 06269, United States

Supporting Information

ABSTRACT: Visual pigments have a conserved phenylalanine in transmembrane helix 5 located near the β-ionone ring of the retinal chromophore. Site-directed mutants of this residue (F207) in a short-wavelength sensitive visual pigment (VCOP) were studied using UV−visible spectroscopy to investigate its role in photosensitivity and formation of the light-activated state. The side chain is important for pigment formation: VCOP^{F207A}, VCOP^{F207L}, VCOP^{F207M}, and VCOP^{F207W} substitutions all bound 11-*cis*-retinal and formed a stable visual pigment, while VCOP^{F207V}, VCOP^{F207S}, VCOP^{F207T}, and VCOP^{F207Y} substitutions do not. The extinction coefficients of all pigments are close, ranging between 35800 and 45600 M^{-1} cm^{-1}. Remarkably, the mutants exhibit an up to 5-fold reduction in photosensitivity and also abnormal photobleaching behavior. One mutant, VCOP^{F207A}, forms an isomeric composition of the retinal chromophore after illumination comparable to that of wild-type VCOP yet does not release the all-*trans*-retinal chromophore. These findings suggest that the conserved F207 residue is important for a normal photoactivation pathway, formation of the active conformation and the exit of all-*trans*-retinal from the chromophore-binding pocket.

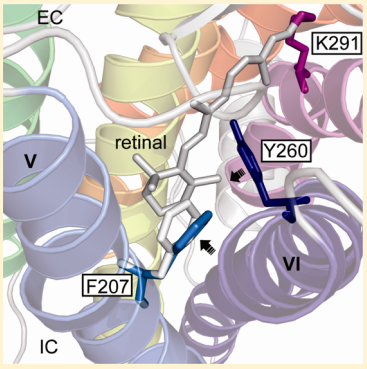

Vertebrate visual pigments absorb light, which causes the isomerization of the covalently bound ligand, 11-*cis*-retinal, to an all-*trans* conformation (for a recent review, see ref 1). The chromophore is attached via a Schiff base linkage between the chromophore and a conserved lysine residue in transmembrane helix 7 and is stabilized by a nearby acidic residue. Following isomerization, the stored energy of the absorbed photon drives structural changes in the visual pigment through a series of transient photointermediate states, which are stable over a limited time and temperature range.[2,3] This thermal relaxation of the primary photointermediate leads to the formation of the active state, meta II.[4] Once in the meta II state, the visual pigment can bind and activate G proteins, which in turn initiate the phototransduction cascade in the retina.[5] Visual pigments have a higher photosensitivity than the chromophore alone in solution.[6−8] When 11-*cis*-retinal is bound to rod opsin, its extinction coefficient and quantum yield of isomerization are increased by ∼1.7- and ∼4-fold, respectively, versus those of the free chromophore.[6−8] The rod and cone visual pigments have similar photosensitivities, differing by <20%.[9−11] These findings suggest that conserved features within the transmembrane domain, specifically the interactions between the chromophore and key binding site residues of the protein, contribute to the high photosensitivity of visual pigments. Currently, there is limited understanding of the molecular determinants underlying photosensitivity. Substitutions of the primary counterion of the retinal Schiff base result in a decreased quantum yield of isomerization and suggest that this conserved residue plays a role in visual pigment photosensitivity.[9,10,12,13] Moreover, a covalent Schiff base linkage is crucial for the efficient formation and stabilization of the active meta II state.[14] While additional residues within the retinal-binding pocket of rhodopsin are required for a normal photoactivation pathway,[1] at present the exact mechanisms are not known. Moreover, there is limited information about cone visual pigments (e.g., refs 15 and 16).

In this study of the *Xenopus* short-wavelength sensitive cone opsin (VCOP), we investigated conserved residues near the β-ionone ring of the retinal chromophore, opposite to the Schiff base linkage, focusing on photosensitivity. We used a homology model of VCOP to predict residues in this region [TM5 and TM6 (Figure 1)]. In the three receptors examined, both intracellular and extracellular ends of the helices are closely apposed, while the middle of TM6 has a bulge around a conserved proline (Figure 1). This creates a potential region for retinal to move between the interior of the helical bundle and the surrounding lipid.[17,18] Notably, opposite from the conserved proline is a conserved phenylalanine (VCOP^{F207}, RHO^{F212}, and βAR2^{F208}). In the VCOP model, the phenyl moiety is rotated toward the ligand-binding pocket, while in the other receptors, it is rotated toward the membrane bilayer. Supporting the potential role of this region are studies of

Received: April 19, 2013
Revised: June 30, 2013
Published: July 1, 2013

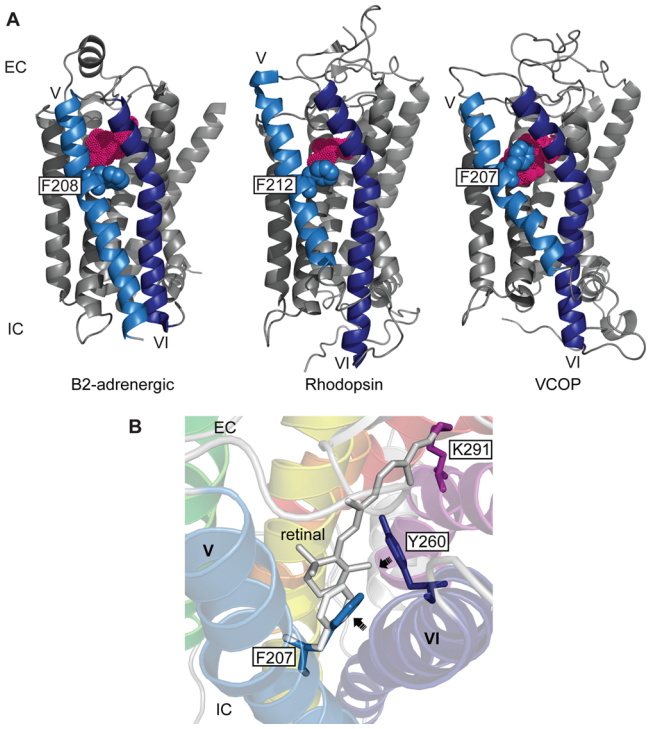

Figure 1. (A) Ribbon diagrams of the β2-adrenergic receptor (Protein Data Bank entry 3NY8[43]) and bovine rhodopsin (Protein Data Bank entry 1U19[18]) for crystal structures and the homology model of *Xenopus* violet cone opsin (VCOP[44,45]). Helices 5 and 6 are colored blue and dark blue, respectively. Residue F207 is depicted in space filling mode. Densities of the inverse agonists are shown as pink dots. (B) Binding pocket of VCOP. The homology model shows putative changes during VCOP activation. Movement of residues is shown by a dashed arrow. Residues F207 in helix V, Y260 in helix VI, and K291 in helix VII are depicted, as is 11-*cis*-retinal. The dark state rotamer is colored blue for position F207, while a possible rotamer in the active state is colored white (see Discussion).

rhodopsin and parapinopsin that showed that mutations is this region can cause spectral shifts in the meta II state, and changes in G protein activation were observed.[19] This observation led to the suggestion that there is a pivot in this region that is required for the formation of the G protein-activating state of these two rhodopsins. To explore the potential functional role of F207 in cone visual pigment photosensitivity, we used site-specific substitutions and UV−visible (UV−vis) spectroscopy to characterize photoactivation. We show that several substitutions significantly perturb photosensitivity and lead to abnormal photobleaching. Thus, we suggest this aromatic residue participates in the formation of meta II and the release of all-*trans*-retinal from short-wavelength sensitive visual pigments.

MATERIALS AND METHODS

Visual Pigment Expression and Purification. The epitope-tagged VCOP plasmids used for site-directed mutagenesis and protein expression have been described previously.[12] The mutants were expressed in COS1 cells by transient transfection, purified by immunoaffinity chromatography, and analyzed as previously described.[12] COS1 cells expressing visual pigments were mixed overnight with 5 μM 11-*cis*-retinal [provided by the National Eye Institute (NEI)] at 4 °C. Pigments were eluted in 50 mM HEPES, 140 mM NaCl, 3 mM $MgCl_2$ (pH 6.6), 0.1% *N*-dodecyl β-D-maltoside, and 20% glycerol and concentrated by ultrafiltration centrifugation (Amicon Utracel30K, Millipore). Transfections and purifications were performed at least twice for each mutant visual pigment.

UV−Visible Spectroscopy. UV−visible absorption spectra of the visual pigments were obtained using a spectrophotometer (Beckman DU 640 or Cary 50) equipped with a water-jacketed cuvette holder. Spectra from samples containing ~1 μg of visual pigment in 10 mM MES containing 0.1% dodecyl maltoside (pH 6.0) were first collected under dark conditions. Samples were irradiated with an LED array (Lamina Lighting Titan LED light engine, model NT-53F0-0428 RGB, operating the blue channel at 460−470 nm and ~25.4 mW), and spectra were recorded after different lengths of time. The photometric curves, i.e., amount of pigment remaining at a given time following irradiation, were calculated from the averaged absorbance values between 445 and 450 nm, constrained normalized to the initial value (100) and the final value (0) after delivery of 3.9×10^{18} photons. The resulting curves were fit to the following equation:

$$A(n) = A_0 e^{-\gamma n}$$

where $A(n)$ is the absorbance after the delivery of n photons, A_0 is the initial absorbance before illumination, and γ is related to the photosensitivity of the pigment. Each point represents the average of three experiments. For light−dark difference spectra, light scattering was corrected using $1/\lambda^4$. Spectra were normalized at 280 nm, subtracted, and smoothed using a smoothing kernel (SigmaPlot11, Jandel Scientific).

High-Performance Liquid Chromatography (HPLC) Analysis. For the photobleaching experiments prior to chromophore extractions, 50 μg of pigment in 3.3 mL of 10 mM MES (pH 6.0) and 0.1% dodecyl maltoside was illuminated using an LED array (480 μW) for a total of 131 s at 10 °C. After illumination, the protein samples were transferred to ice. All extraction procedures were performed under dim red light using ice-cold solvents. Then, 250 μL of 1 M NH_2OH-HCl (pH 6.5) and 1.7 mL of methanol were added. The samples were vortexed, incubated on ice for 10 min, transferred to a separatory funnel, and mixed sequentially with methanol (1.7 mL), dichloromethane (3.3 mL), and hexane (16.5 mL). The aqueous layer was extracted twice more, and organic layers pooled and evaporated under N_2. Retinal oxime standards, 11-*cis*-retinal (gift of NEI), all-*trans*-retinal (Sigma-Aldrich), and 9-*cis*-retinal (Sigma-Aldrich), were extracted in parallel. All retinal extracts were dissolved in hexane for HPLC analysis. All solvents were HPLC grade (Fisher). A portion of the hexane layer (50 μL) was injected into an HPLC system equipped with two HPLC columns (Waters Prep Nova-Pak HR silica columns, 3.9 mm × 300 mm, Waters catalog no. WAT038501) and a Waters 2487 dual-wavelength absorbance detector monitoring at 360 nm. The mobile phase used to separate the chromophores consisted of 96% hexane, 3% *tert*-butyl methyl ether, 0.5% 1-octanol, and 0.5% 1,4-dioxane. All solvents used were HPLC grade (Fisher). The flow rate was set to 2.5 mL/min. Retinal oxime standards (all-*trans*-, 11-*cis*-, and 9-*cis*-retinal oxime) were used to assign the retention times of the peaks observed. The percent retinal isomer formed was calculated by integrating the area under each peak using the iPeak plugin (http://terpconnect.umd.edu/~toh/spectrum/TOC.html) for MatLab. Our low temperature and concentrations favor formation of the *syn* oxime enantiomers, and while the *anti* enantiomers were observed, these bands

dx.doi.org/10.1021/bi400490g | *Biochemistry* 2013, 52, 5084−5091

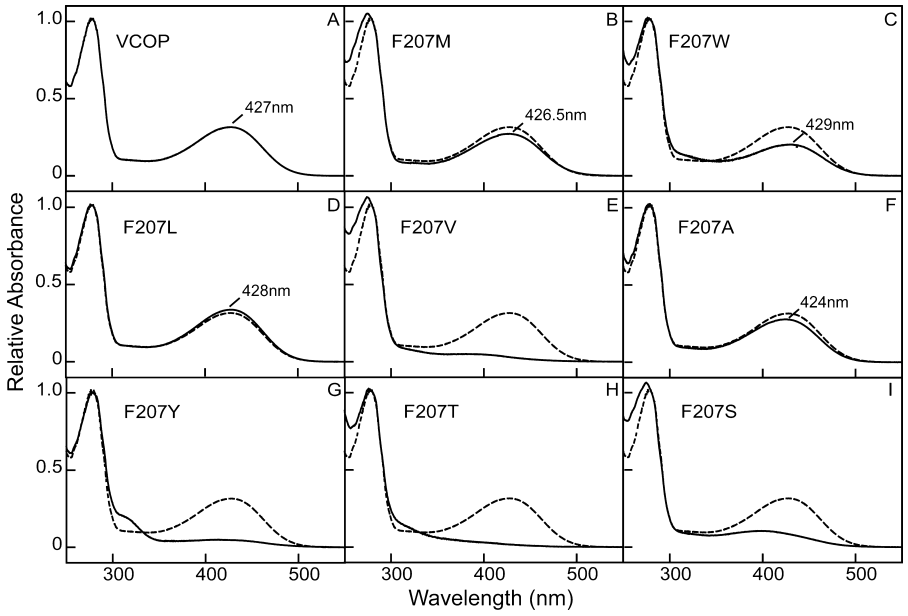

Figure 2. Dark spectra of purified VCOP and VCOP^{F207} mutant visual pigments. In mutant spectra, the spectrum for VCOP is shown as a dashed line and the spectrum for the mutant as a solid line. λ_{max} is shown for visual pigments with a chromophore peak. The spectra were normalized to A_{280}.

appeared at longer retention times and were broad and difficult to characterize. The *syn* peaks were used exclusively for assigning the isomeric concentrations. The following extinction coefficients at 360 nm were used: 29600 M^{-1} cm^{-1} for 11-*cis*-retinal, 51600 M^{-1} cm^{-1} for all-*trans*-retinal, and 30600 M^{-1} cm^{-1} for 9-*cis*-retinal.[7] Three independent experiments were performed.

Acid Denaturation. The visual pigment was diluted to 1 μg in 10 mM MES buffer and 0.1% dodecyl maltoside (pH 6.0) at 10 °C. Spectra were recorded before and after addition of H_2SO_4 to bring the pH to 1.8. Averaged spectra were used to determine the A_{425}/A_{440} ratio, and final spectra were smoothed using a kernel (Sigma Plot). The concentrations of the chromophore were determined using an extinction coefficient at 440 nm of 30800 M^{-1} cm^{-1}.[20] The extinction coefficients were determined from three separate preparations.

RESULTS

Dark Absorption Spectra. We prepared eight amino acid substitutions at position 207 in VCOP and expressed these mutants in a well-established heterologous COS1 system. Following incubation with 11-*cis*-retinal, the mutants were purified and characterized by UV−visible spectroscopy. VCOP and four of the mutants (VCOP^{F207M}, VCOP^{F207W}, VCOP^{F207L}, and VCOP^{F207A}) exhibited a chromophore peak, indicating that the receptor was able to bind the ligand 11-*cis*-retinal (Figure 2A−D,F). However, mutants VCOP^{F207V}, VCOP^{F207Y}, VCOP^{F207T}, and VCOP^{F207S} exhibited little or no chromophore peak, suggesting the mutant was not properly folded or did not stably bind 11-*cis*-retinal (Figure 2E,G−I). This observation suggests that F207 has steric constraints that must be met for the formation of a native retinal-binding pocket. The wild-type pigment has a λ_{max} of 427 nm,[21] and the values of the mutant pigments were similar, although there were small shifts depending upon the substitution (Table 1). These four mutants also folded well, as judged by the $A_{280}/A_{\lambda_{max}}$ ratio. We measured the extinction coefficients at λ_{max} mutants using acid denaturation.[20] This process causes the absorption maximum to shift from 427 to 440 nm. All of mutants had extinction coefficients quite similar to that of the wild-type protein, ranging from 35800 to 45600 M^{-1} cm^{-1} (Table 1). We note that mutant VCOP^{F207A} has an extinction coefficient slightly higher than those of the rest of the mutants. In summary, we conclude that if the steric constraints at F207 are accommodated, the protein forms a fairly normal 11-*cis*-retinal-binding pocket (i.e., does not have significantly altered spectral tuning) and that the protein is stable in the dark.

Table 1. Spectroscopic Properties of VCOP Mutants

pigment	$A_{280}/A_{\lambda_{max}}$	λ_{max}[a] (nm)	ε[b] (M^{-1} cm^{-1})	relative photosensitivity[d]
VCOP	3.4	427	39500 ± 2000	1
F207A	3.9	424	45600 ± 3000	0.24 ± 0.05
F207L	3.0	428	38700 ± 500	0.60 ± 0.23
F207M	3.8	427	35800 ± 3000	0.26 ± 0.05
F207W	4.6	429	nd[c]	0.21 ± 0.02

[a]Wavelength of maximum absorbance ±1 nm after removal of light scattering with correction factor $1/\lambda^4$. [b]Based on the extinction coefficient of the protonated Schiff base of retinal.[20] [c]Not determined. [d]Slopes of the single exponential in Figure 6 were used to compare mutants to VCOP, which was set to 1.0. The variation of the VCOP slope is ±0.06.

Photoisomerization of the VCOP^{F207A} Retinal Chromophore. We investigated the photosensitivity of the VCOP^{F207A} mutant that bound 11-*cis*-retinal. Visual pigment samples were exposed to light, and then the retinal chromophores were extracted for isomeric analysis (Figure 3). The light−dark difference spectrum of VCOP shows the expected loss of the 11-*cis*-retinal chromophore peak and the increase in absorbance at 380 nm from all-*trans*-retinal formation.[21] Because this experiment was performed at 10 °C, the majority of the photoproduct is meta II.[22] By contrast, the VCOP^{F207A} mutant pigment has an altered difference spectrum, with a broad peak centered at 380 nm and a small positive red shoulder. Analysis of the chromophore extracted from these pigments showed that 11-*cis*-retinal in both VCOP

dx.doi.org/10.1021/bi400490g | *Biochemistry* 2013, 52, 5084−5091

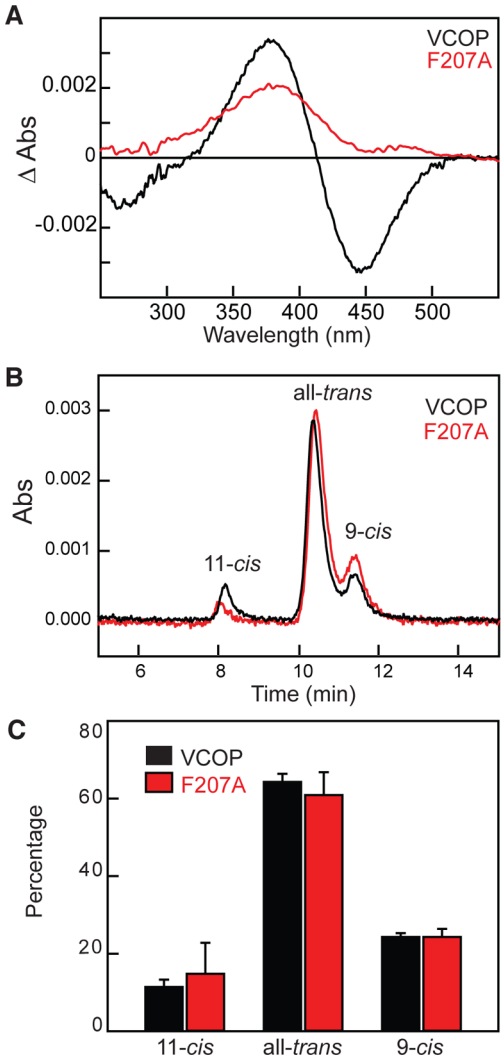

Figure 3. Extent of retinal isomerization after illumination in VCOP and F207 mutant pigment. (A) UV−vis absorbance spectra were recorded before and after illumination (4.1×10^{16} photons) of visual pigments at 10 °C. The absorbance spectrum obtained after illumination was subtracted from the absorbance spectrum obtained in the dark, and the resulting difference spectrum is shown. (B) HPLC patterns of wild-type VCOP and VCOP^{F207A}. (C) Isomeric mixture of the extracted chromophore from illuminated samples as quantified by HPLC (error bars are standard deviations; $n = 3$).

and VCOP^{F207A} underwent similar conversion to all-*trans* and 9-*cis* isomers following exposure to light, with no statistical difference in overall conversion (Figure 3). Thus, although both VCOP and VCOP^{F207A} efficiently absorb light to form similar amounts of photoactivated pigment, there are dramatic differences in the spectral states following isomerization in the mutant protein.

Abnormal Photoactivation Pathway in VCOP^{F207} Mutant Pigments. VCOP rapidly formed a stable photostationary state at 10 °C, consisting primarily of meta II (Figure 3A).[21,22] By contrast, VCOP^{F207A} formed an unusually metastable photointermediate immediately after illumination, with a photostationary state with a λ_{max} of ∼415 nm that was similar to VCOP, even though the photoactivating light intensity was sufficient to isomerize the same fraction of the VCOP^{F207A} pigment as in VCOP. There was a very slow (>30 min) blue shift in VCOP^{F207A} (Figure 4). Intense illumination of VCOP^{F207A} produced a photointermediate similar to meta II of VCOP, suggesting that multiple-photon absorption is necessary to rapidly convert VCOP^{F207A} to meta II.

We obtained photometric curves for VCOP and the VCOP^{F207} mutants. Spectra were recorded after successive flashes, with ∼1 min between flashes, during which time there were minimal changes in the photointermediate spectra (Figure 4). Thus, the photons delivered to each sample were cumulative. In VCOP, there was a progressive loss of absorbance at the 427 nm peak and an increase at 380 nm, corresponding to meta II (Figure 5A). The difference spectra of VCOP show a single isosbestic point at 410 nm indicating a single-step conversion from the dark to meta II.[21,23] By contrast, the VCOP^{F207} mutants were very resistant to photoconversion to meta II in this photon range (Figure 5B−E). The F207 mutant spectra do not exhibit a single isosbestic point, suggesting that multiple photointermediates exist at 10 °C. To determine whether the thermal transition temperature for the conversion from one of the photoactivation intermediates (e.g., meta I) to meta II is altered by the mutation, we illuminated the VCOP^{F207A} pigment at 30 °C (Figure 5F). However, only slight differences in the VCOP^{F207A} spectra were seen compared to that recorded at 10 °C. Photometric curves were used to calculate and compare differences in photosensitivity (Figure 6). The curves from all of the mutants had significantly reduced slopes compared to that of VCOP (the same VCOP data are used for comparison with each VCOP mutant), with VCOP^{F207L} having a 2-fold reduction and the others having ∼5-fold reductions. Thus, the

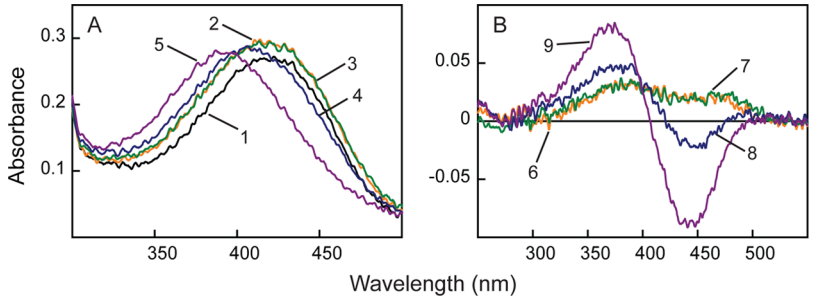

Figure 4. Stability of photoactivated VCOP^{F207A} at 10 °C. The UV−vis absorbance (A) spectra for VCOP^{F207A} were recorded at 10 °C. All spectra were then subtracted from the first dark spectrum (B). An initial dark recording was taken; then samples were illuminated with 6.6×10^{16} photons, and spectra were recorded 0, 1, and 30 min afterward (2−4, corresponding to 6−8, respectively). Finally, samples were exposed to light (2×10^{18} photons) again, and a final spectrum was recorded (5 and 9).

dx.doi.org/10.1021/bi400490g | *Biochemistry* 2013, 52, 5084−5091

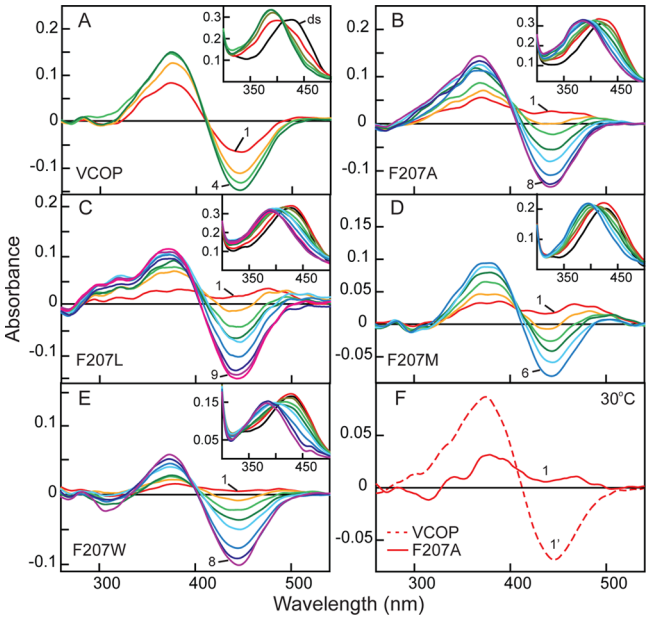

Figure 5. Stability of photoactivated VCOP^{F207A} mutants. Light−dark difference spectra of visual pigment samples at 10 °C (A−E) were recorded and then successively illuminated with the following total number of photons: 3.3×10^{16} (red), 6.6×10^{16} (orange), 9.8×10^{16} (green), 1.3×10^{17} (dark green), 1.6×10^{17} (aqua), 3.3×10^{17} (blue), 6.6×10^{17} (dark blue), 2×10^{18} (purple), and 4×10^{18} (magenta). Insets show the absorbance spectra. (F) Light−dark difference spectra from photobleaching experiments (3.3×10^{16} photons) were recorded at 30 °C with VCOP and VCOP^{F207A}.

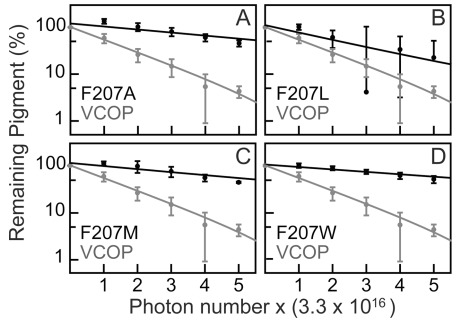

Figure 6. Photobleaching of VCOP and F207 mutant pigments. Pigments were successively photobleached at 10 °C with the indicated number of photons. Amounts of remaining pigment were determined as described in Materials and Methods. The same data for wild-type VCOP are colored gray in each panel. Mutant data are colored black. Dots represent the average of three experiments, and the error bars show the standard deviation. The solid line is the exponential fit to the mean of the data collected for each pigment.

F207 residue is critical to the photosensitivity of this short-wavelength visual pigment.

DISCUSSION

In this study, we examine the influence of the F207 residue on the photosensitivity of cone visual pigment VCOP. Because the β-ionone ring of retinal has been shown to play a major role in visual pigment activation,[1,24−26] we tested the hypothesis that nearby conserved residues will also be necessary for the formation of meta II. In the dark state, noncovalent interactions of the β-ionone ring and F207 were shown in rhodopsin by nuclear magnetic resonance (NMR).[27] Upon isomerization, these interactions are potentially altered in the formation of the active state. Thus, we focused on one conserved phenylalanine in TM5, VCOP^{F207}. Not all substitutions at F207 were tolerated, while others produced visual pigments with λ_{max} values and extinction coefficients very similar to those of VCOP. For mutants that formed little to no chromophore peak, it is possible that the protein did not fold properly or did not stably bind retinal. In the case of F207V, this substitution may affect helix formation or the orientation as other short chain or branched amino acids are tolerated. Moreover, the replacement of F207 with a hydroxyl-bearing residue may result in new interactions that could restrict retinal binding. For example, a hydrogen bond between the hydroxyl side chain at position 207 and TM6 could disrupt the helical spacing and thereby limit access in the binding pocket for the β-ionone ring. Thus, as long as steric constraints for helical packing are satisfied, F207 may not play a direct role in the 11-*cis*-retinal-binding pocket. This observation agrees with studies of rhodopsin and parapinopsin, which proposed that this region was primarily important for agonist (i.e., all-*trans*-retinal) but not inverse agonist (11-*cis*-retinal) binding.[19] However, in the case of VCOP, there were dramatic decreases in photosensitivity and apparently abnormal photointermediate formation. Such altered bleaching phenotypes have been reported previously in rhodopsin (G90D, A292, and F265).[28,29] Further experiments will be needed to investigate mechanisms that could relate these results to our study.

Our results suggest that the normal photoactivation pathway (batho → lumi → meta I → meta II)[22] is defective in one or more steps in the VCOP^{F207} mutants. This observation is represented by an elevation of one or more of the thermal barriers between the photointermediate states (Figure 7). Because we have not been able to assign a specific intermediate that is affected by the mutation, we represent the mutant photointermediate state(s) by $I_{all\text{-}trans}$. In this model, the photoactivated mutant pigment accumulates in the $I_{all\text{-}trans}$ intermediate, which has a slow thermal transition to the meta II intermediate. We also hypothesize that the normal pathway is accessible at a significantly reduced efficiency. This model explains the reduced photosensitivity, the abnormal UV−visible spectra, and the effect of intense light on the photosensitivity of VCOP^{F207} mutant pigments. The broad absorbance peak associated with $I_{all\text{-}trans}$ at a λ greater than ∼400 nm further suggests that the Schiff base is protonated in this intermediate. The photoisomerization yields of the VCOP^{F207} mutant chromophores are quite similar to those of VCOP, and the chromophore absorbance peak is blue-shifted, implying that the primary photointermediate, batho, is not affected by the mutations. Thus, we suggest that one or more of the lumi → meta I → transitions are affected by the mutation of F207 during active state formation in a cone visual pigment. Studies of the comparable amino acid residue in bovine rhodopsin showed that the level of G protein activation was decreased by 25%,[19] consistent with a defect in the photoactivation pathway.

Insight into the structural impact of F207 is provided by studies of rhodopsin, with attention paid to the changes occurring at the β-ionone ring, at transmembrane helix 5, and in interactions between the two during activation. In the lumi rhodopsin structure, the β-ionone ring is both relaxed and translated in comparison to that of batho.[30] Specifically, it was proposed that the β-ionone ring moves toward helix 5 near position F212 upon activation by NMR,[31,32] causing a steric clash between the β-ionone ring and residues of helix 5 that

dx.doi.org/10.1021/bi400490g | *Biochemistry* 2013, 52, 5084−5091

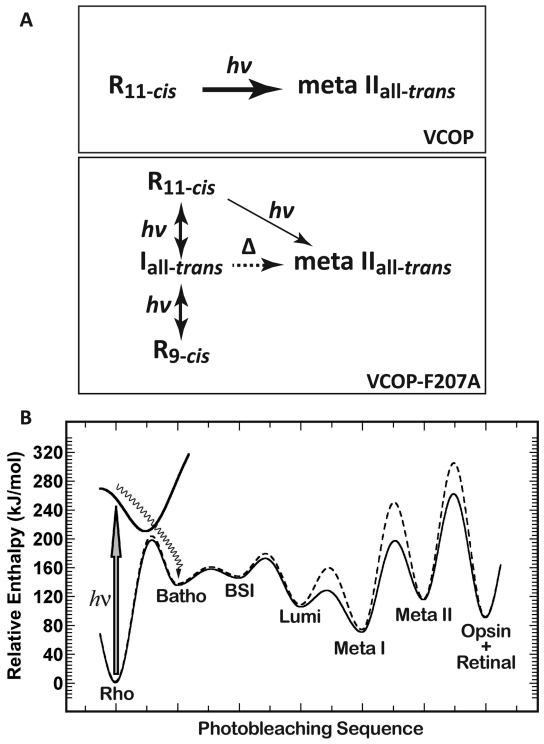

Figure 7. (A) Abnormal photobleaching pathway in the VCOP^{F207} mutant pigments at 10 °C. The main photoproduct of VCOP illuminated with smaller amounts of light is meta II (top). With the VCOP^{F207A} mutant, the predominant photoproduct is not meta II, but a mixture of intermediates (bottom). It requires many more photons to convert VCOP^{F207A} to meta II. The visual pigment with the 11-*cis* chromophore is labeled $R_{11\text{-}cis}$ and that with the 9-*cis* chromophore $R_{9\text{-}cis}$. Absorption of a photon results in the isomerization of 11-*cis*-retinal to all-*trans* and either meta II or intermediate $I_{all\text{-}trans}$. Thermal changes are indicated by Δ. (B) Energy diagram for the transition from the dark-adapted visual pigment to the light-activated forms (R*). The rhodopsin energies have been used and for illustration have arbitrarily increased VCOP^{F207A} barriers by ∼10 kJ/mol. The VCOP^{F207} mutants are proposed to have an increased thermal barrier to transition, thus reducing the photosensitivity. For the sake of simplicity, the dark state is labeled as Rho to represent the 11-*cis* pigment and 9-*cis* pigments are not included in this figure. See Discussion for more details.

leads to the rotation and elongation of helix 5 and changes in interhelical hydrogen bonding of meta II.[4,18,31,33] Thus, changes in helix 5 likely occur in meta I or in the transition to meta II, during which time a counterion switch is observed.[33−35] Coupled to this transition are Schiff base deprotonation, rotation of helix 6, and proton uptake, all of which are necessary for the formation of the G protein activating state of meta II.[4,36,37] Together, these coordinated structural changes comprise the pivot activation mechanism for visual pigments.[4,18,30,38] In general, our results agree with the importance of structural changes in the interface between helices 5 and 6. In fact, it is possible that the VCOP^{F207} mutations block the pivot. Thus, F207 could undergo a rotameric switch coupled to β-ionone ring rotation, providing an energy coupling mechanism to provide high photosensitivity for formation of the active state and rapid release of all-*trans*-retinal from cone visual pigments.

Interestingly, F207 may be acting with another conserved residue as part of a switch or pivot leading to receptor activation. One such residue in VCOP is Y260$^{6.48}$, part of the conserved CWxP motif in helix 6. In rhodopsin and the β2-adrenergic receptor, there is a Trp residue at this position that has been postulated to rotate during receptor activation, and thus, the mechanism is termed the rotamer toggle switch in G protein-coupled receptors (GPCRs).[39,40] Molecular dynamics simulations showed rotation of W265$^{6.48}$ toward F208 in the β2-adrenergic receptor, where stable aromatic stacking interactions were seen between these residues in the active state.[41] This observation suggests that F207 may stabilize the active rotamer of W265 to promote active state receptor formation. Mutational analysis of these residues supports this as substitutions at these positions in nonvisual pigment GPCRs reduced the level of or eliminated agonist-induced signaling but did not impair ligand binding.[41] A role for F207 in GPCR activation has been shown in the gherlin, NK1, and β2-adrenergic receptors.[41]

■ CONCLUSION

Our study provides the first demonstration of the role of F207 in the activation of a cone visual pigment. While F207 is conserved in rhodopsin, it is not clear if this residue alters the release of all-*trans*-retinal or just the meta I−meta II equilibrium.[19] It is, however, possible that VCOP^{F207} acts specifically in the regulation of short-wavelength sensitive cone photosensitivity. Because a phenylalanine is absent from the human L/M cone opsins,[42] other residues in this vicinity may be required to achieve high photosensitivity and, coupled to that, active state formation. To understand the mechanisms underlying visual pigment photosensitivity and activation, it will be necessary to determine what other residues regulate these crucial functions.

■ ASSOCIATED CONTENT

Supporting Information

Absorbance spectra from the acid denaturation experiments. This material is available free of charge via the Internet at http://pubs.acs.org.

■ AUTHOR INFORMATION

Corresponding Author

*B.E.K.: 750 E. Adams St., Syracuse, NY 13210; e-mail, knoxb@upstate.edu; telephone, (315) 464-8719; fax, (315) 464-8750. R.R.B.: Department of Chemistry, University of Connecticut, Storrs, CT 06269; e-mail, rbirge@uconn.edu; telephone, (860) 486-6720; fax, (860) 486-2981.

Funding

This work was supported in part by National Institutes of Health Grants EY-11256 and EY-12975 (B.E.K.) and GM-34548 (R.R.B.), Research to Prevent Blindness (Unrestricted Grant to SUNY Upstate Medical University Department of Ophthalmology), the Harold S. Schwenk Sr. Distinguished Chair in Chemistry at the University of Connecticut, and the Lions of CNY.

Notes

The authors declare no competing financial interest.

■ ACKNOWLEDGMENTS

We thank E. Solessio for helpful discussions and J. Chen and S. Reks for their assistance with cell culture and mutagenesis.

REFERENCES

(1) Smith, S. O. (2010) Structure and activation of the visual pigment rhodopsin. *Annu. Rev. Biophys. 39*, 309−328.

(2) Lewis, J. W., and Kliger, D. S. (1992) Photointermediates of visual pigments. *J. Bioenerg. Biomembr. 24*, 201−210.

(3) Vought, B. W., Dukkipatti, A., Max, M., Knox, B. E., and Birge, R. R. (1999) Photochemistry of the primary event in short-wavelength visual opsins at low temperature. *Biochemistry 38*, 11287−11297.

(4) Choe, H. W., Kim, Y. J., Park, J. H., Morizumi, T., Pai, E. F., Krauss, N., Hofmann, K. P., Scheerer, P., and Ernst, O. P. (2011) Crystal structure of metarhodopsin II. *Nature 471*, 651−655.

(5) Hofmann, K. P., Scheerer, P., Hildebrand, P. W., Choe, H. W., Park, J. H., Heck, M., and Ernst, O. P. (2009) A G protein-coupled receptor at work: The rhodopsin model. *Trends Biochem. Sci. 34*, 540−552.

(6) Kropf, A., and Hubbard, R. (1970) The photoisomerization of retinal. *Photochem. Photobiol. 12*, 249−260.

(7) Wald, G., and Brown, P. K. (1953) The molar extinction of rhodopsin. *J. Gen. Physiol. 37*, 189−200.

(8) Dartnall, H. J. (1968) The photosensitivities of visual pigments in the presence of hydroxylamine. *Vision Res. 8*, 339−358.

(9) Tsutsui, K., Imai, H., and Shichida, Y. (2007) Photoisomerization efficiency in UV-absorbing visual pigments: Protein-directed isomerization of an unprotonated retinal Schiff base. *Biochemistry 46*, 6437−6445.

(10) Tsutsui, K., Imai, H., and Shichida, Y. (2008) E113 is required for the efficient photoisomerization of the unprotonated chromophore in a UV-absorbing visual pigment. *Biochemistry 47*, 10829−10833.

(11) Okano, T., Fukada, Y., Shichida, Y., and Yoshizawa, T. (1992) Photosensitivities of iodopsin and rhodopsins. *Photochem. Photobiol. 56*, 995−1001.

(12) Babu, K. R., Dukkipati, A., Birge, R. R., and Knox, B. E. (2001) Regulation of phototransduction in short-wavelength cone visual pigments via the retinylidene Schiff base counterion. *Biochemistry 40*, 13760−13766.

(13) Ramos, L. S., Chen, M. H., Knox, B. E., and Birge, R. R. (2007) Regulation of photoactivation in vertebrate short wavelength visual pigments: Protonation of the retinylidene Schiff base and a counterion switch. *Biochemistry 46*, 5330−5340.

(14) Matsuyama, T., Yamashita, T., Imai, H., and Shichida, Y. (2010) Covalent bond between ligand and receptor required for efficient activation in rhodopsin. *J. Biol. Chem. 285*, 8114−8121.

(15) Shichida, Y., Imai, H., Imamoto, Y., Fukada, Y., and Yoshizawa, T. (1994) Is chicken green-sensitive cone visual pigment a rhodopsin-like pigment? A comparative study of the molecular properties between chicken green and rhodopsin. *Biochemistry 33*, 9040−9044.

(16) Dukkipati, A., Vought, B. W., Singh, D., Birge, R. R., and Knox, B. E. (2001) Serine 85 in transmembrane helix 2 of short-wavelength visual pigments interacts with the retinylidene Schiff base counterion. *Biochemistry 40*, 15098−15108.

(17) Cherezov, V., Rosenbaum, D. M., Hanson, M. A., Rasmussen, S. G., Thian, F. S., Kobilka, T. S., Choi, H. J., Kuhn, P., Weis, W. I., Kobilka, B. K., and Stevens, R. C. (2007) High-resolution crystal structure of an engineered human β2-adrenergic G protein-coupled receptor. *Science 318*, 1258−1265.

(18) Okada, T., Sugihara, M., Bondar, A. N., Elstner, M., Entel, P., and Buss, V. (2004) The retinal conformation and its environment in rhodopsin in light of a new 2.2 Å crystal structure. *J. Mol. Biol. 342*, 571−583.

(19) Tsukamoto, H., Terakita, A., and Shichida, Y. (2010) A pivot between helices V and VI near the retinal-binding site is necessary for activation in rhodopsins. *J. Biol. Chem. 285*, 7351−7357.

(20) Kito, Y., Suzuki, T., Azuma, M., and Sekoguti, Y. (1968) Absorption spectrum of rhodopsin denatured with acid. *Nature 218*, 955−957.

(21) Starace, D. M., and Knox, B. E. (1998) Cloning and expression of a *Xenopus* short wavelength cone pigment. *Exp. Eye Res. 67*, 209−220.

(22) Kusnetzow, A., Dukkipati, A., Babu, K. R., Singh, D., Vought, B. W., Knox, B. E., and Birge, R. R. (2001) The photobleaching sequence of a short-wavelength visual pigment. *Biochemistry 40*, 7832−7844.

(23) Starace, D. M., and Knox, B. E. (1997) Activation of transducin by a *Xenopus* short wavelength visual pigment. *J. Biol. Chem. 272*, 1095−1100.

(24) Okada, T., Kandori, H., Shichida, Y., Yoshizawa, T., Denny, M., Zhang, B. W., Asato, A. E., and Liu, R. S. (1991) Spectroscopic study of the batho-to-lumi transition during the photobleaching of rhodopsin using ring-modified retinal analogues. *Biochemistry 30*, 4796−4802.

(25) Jager, F., Jager, S., Krutle, O., Friedman, N., Sheves, M., Hofmann, K. P., and Siebert, F. (1994) Interactions of the β-ionone ring with the protein in the visual pigment rhodopsin control the activation mechanism. An FTIR and fluorescence study on artificial vertebrate rhodopsins. *Biochemistry 33*, 7389−7397.

(26) Bartl, F. J., Fritze, O., Ritter, E., Herrmann, R., Kuksa, V., Palczewski, K., Hofmann, K. P., and Ernst, O. P. (2005) Partial agonism in a G protein-coupled receptor: Role of the retinal ring structure in rhodopsin activation. *J. Biol. Chem. 280*, 34259−34267.

(27) Creemers, A. F., Kiihne, S., Bovee-Geurts, P. H., DeGrip, W. J., Lugtenburg, J., and de Groot, H. J. (2002) ^{1}H and ^{13}C MAS NMR evidence for pronounced ligand-protein interactions involving the ionone ring of the retinylidene chromophore in rhodopsin. *Proc. Natl. Acad. Sci. U.S.A. 99*, 9101−9106.

(28) Rao, V. R., Cohen, G. B., and Oprian, D. D. (1994) Rhodopsin mutation G90D and a molecular mechanism for congenital night blindness. *Nature 367*, 639−642.

(29) Dryja, T. P., Berson, E. L., Rao, V. R., and Oprian, D. D. (1993) Heterozygous missense mutation in the rhodopsin gene as a cause of congenital stationary night blindness. *Nat. Genet. 4*, 280−283.

(30) Nakamichi, H., and Okada, T. (2006) Local peptide movement in the photoreaction intermediate of rhodopsin. *Proc. Natl. Acad. Sci. U.S.A. 103*, 12729−12734.

(31) Ahuja, S., Crocker, E., Eilers, M., Hornak, V., Hirshfeld, A., Ziliox, M., Syrett, N., Reeves, P. J., Khorana, H. G., Sheves, M., and Smith, S. O. (2009) Location of the retinal chromophore in the activated state of rhodopsin*. *J. Biol. Chem. 284*, 10190−10201.

(32) Patel, A. B., Crocker, E., Eilers, M., Hirshfeld, A., Sheves, M., and Smith, S. O. (2004) Coupling of retinal isomerization to the activation of rhodopsin. *Proc. Natl. Acad. Sci. U.S.A. 101*, 10048−10053.

(33) Ahuja, S., Hornak, V., Yan, E. C., Syrett, N., Goncalves, J. A., Hirshfeld, A., Ziliox, M., Sakmar, T. P., Sheves, M., Reeves, P. J., Smith, S. O., and Eilers, M. (2009) Helix movement is coupled to displacement of the second extracellular loop in rhodopsin activation. *Nat. Struct. Mol. Biol. 16*, 168−175.

(34) Birge, R. R., and Knox, B. E. (2003) Perspectives on the counterion switch-induced photoactivation of the G protein-coupled receptor rhodopsin. *Proc. Natl. Acad. Sci. U.S.A. 100*, 9105−9107.

(35) Yan, E. C., Kazmi, M. A., Ganim, Z., Hou, J. M., Pan, D., Chang, B. S., Sakmar, T. P., and Mathies, R. A. (2003) Retinal counterion switch in the photoactivation of the G protein-coupled receptor rhodopsin. *Proc. Natl. Acad. Sci. U.S.A. 100*, 9262−9267.

(36) Arnis, S., Fahmy, K., Hofmann, K. P., and Sakmar, T. P. (1994) A conserved carboxylic acid group mediates light-dependent proton uptake and signaling by rhodopsin. *J. Biol. Chem. 269*, 23879−23881.

(37) Longstaff, C., Calhoon, R. D., and Rando, R. R. (1986) Deprotonation of the Schiff base of rhodopsin is obligate in the activation of the G protein. *Proc. Natl. Acad. Sci. U.S.A. 83*, 4209−4213.

(38) Nakamichi, H., and Okada, T. (2006) Crystallographic analysis of primary visual photochemistry. *Angew. Chem., Int. Ed. 45*, 4270−4273.

(39) Bhattacharya, S., Hall, S. E., and Vaidehi, N. (2008) Agonist-induced conformational changes in bovine rhodopsin: Insight into activation of G-protein-coupled receptors. *J. Mol. Biol. 382*, 539−555.

(40) Shi, L., Liapakis, G., Xu, R., Guarnieri, F., Ballesteros, J. A., and Javitch, J. A. (2002) β2 adrenergic receptor activation. Modulation of the proline kink in transmembrane 6 by a rotamer toggle switch. *J. Biol. Chem. 277*, 40989−40996.

(41) Holst, B., Nygaard, R., Valentin-Hansen, L., Bach, A., Engelstoft, M. S., Petersen, P. S., Frimurer, T. M., and Schwartz, T. W. (2010) A conserved aromatic lock for the tryptophan rotameric switch in TM-VI of seven-transmembrane receptors. *J. Biol. Chem. 285*, 3973−3985.
(42) Sugihara, M., Fujibuchi, W., and Suwa, M. (2011) Structural elements of the signal propagation pathway in squid rhodopsin and bovine rhodopsin. *J. Phys. Chem. B 115*, 6172−6179.
(43) Wacker, D., Fenalti, G., Brown, M. A., Katritch, V., Abagyan, R., Cherezov, V., and Stevens, R. C. (2010) Conserved binding mode of human β2 adrenergic receptor inverse agonists and antagonist revealed by X-ray crystallography. *J. Am. Chem. Soc. 132*, 11443−11445.
(44) Chen, M. H., Sandberg, D. J., Babu, K. R., Bubis, J., Surya, A., Ramos, L. S., Zapata, H. J., Galan, J. F., Sandberg, M. N., Birge, R. R., and Knox, B. E. (2011) Conserved residues in the extracellular loops of short-wavelength cone visual pigments. *Biochemistry 50*, 6763−6773.
(45) Sandberg, M. N., Amora, T. L., Ramos, L. S., Chen, M. H., Knox, B. E., and Birge, R. R. (2011) Glutamic acid 181 is negatively charged in the bathorhodopsin photointermediate of visual rhodopsin. *J. Am. Chem. Soc. 133*, 2808−2811.